

Defect Features Detected by Acoustic Emission for Flip-Chip CGA/FCBGA/PBGA/FPBGA Packages and Assemblies

Reza Ghaffarian, Ph.D.

Jet Propulsion Laboratory, California Institute of Technology

Pasadena, CA

Reza.Ghaffarian@JPL.NASA.Gov

(818) 354-2059

Abstract

C-mode scanning acoustic microscopy (C-SAM) is a non-destructive inspection technique showing the internal features of a specimen by ultrasound. The C-SAM is the preferred method for finding “air gaps” such as delamination, cracks, voids, and porosity. This paper presents evaluations performed on various advanced packages/assemblies especially flip-chip die version of ball grid array/column grid array (BGA/CGA) using C-SAM equipment. For comparison, representative x-ray images of the assemblies were also gathered to show key defect detection features of the two non-destructive techniques.

Key images gathered and compared are:

- Compare the images of 2D x-ray and C-SAM for a plastic LGA assembly showing features that could be detected by either NDE technique. For this specific case, x-ray was a clear winner.
- Evaluate flip-chip CGA and FCBGA assemblies with and without heat sink by C-SAM. Evaluation was to evaluate defect condition of underfill and bump quality. Cross-sectional microscopy performed to compare defect features detected by C-SAM.
- Analyze a number of fine pitch PBGA assemblies by C-SAM to detect the internal features of the package assemblies and solder joint failure at either package or board levels.
- Twenty times touch up by solder iron having 700°F, each with 5-7seconds and induced defects were analyzed by C-SAM images.

Key words: Acoustic microscopy, AE, AMI, C-SAM, FCBGA, FC-CGA, real time x-ray, 2D x-ray, Column grid array, CGA

1.0 ACOUSTIC EMISSION TECHNOLOGY

1.1 Electronic Packaging Trend

Previous generations of microelectronic packaging technology aimed mostly at meeting the needs of high-reliability applications, such as the ceramic leaded quad flat package (CQFP). Nondestructive wire bond pull at the package level and subsequent visual inspection for solder joint integrity at the board level were adequate for ensuring the quality of CQFPs. Consumer electronics are now driving miniaturization trends for electronic packaging and assembly; they introduce a vast number of area array packages. The array packages initially only had hidden solder joints under the bottom area of the package; now the flip-chip die within package also have hidden joints.

The hidden joints—both at package and assembly levels—added significant challenges to the inspectability and certainty of assuring integrity at the various microelectronics hierarchy levels. Another added complexity is the transition to using only Pb-free solder alloys. Suppliers of electronics packages either have or will soon transition to using Pb-free alloys in order to enforce restrictions on hazardous substances (ROHS) for electronic systems. The solder joint appearance for the Pb-free solder alloys is dull rather than shiny, as it is for the tin-lead eutectic solder, which will add confusion even if visual inspection is used inadvertently as a criterion for the quality of joint acceptance or rejection.

Inspection of ball grid array (BGA) and column grid array (CGA) package/assembly, especially their flip-chip versions is challenging [1-5]. Nondestructive x-ray inspection became a new approach for ensuring the quality of area array packages and assemblies. Even though x-ray can detect the level of voids and bridges of solder joints hidden under packages, it become of less value for detecting solder attachment and underfill integrity of higher I/O (>1000 I/Os) packages with flip-chip die

technology (such as FCBGA and FC-CGA; see Figure 1). Ceramic substrates considered for high-reliability applications are heavier and less penetrable to x-ray radiation than plastic, making them even more difficult to inspect for this category of packages and assemblies.

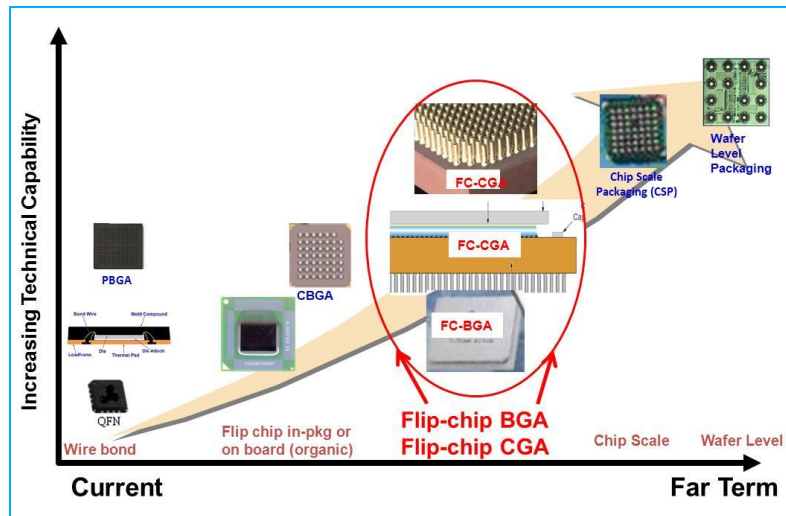


Figure 1. Microelectronic trends for single packaging technologies including flip-chip BGA and CGA.

1.2 Acoustic Micro-imaging, C-SAM, and X-ray

Acoustic microscopes emit ultrasounds ranging from 5 MHz to more than 400 MHz, so that micrometer size resolution can be achieved [6]. Ultrasound that penetrates a sample may be scattered, absorbed or reflected by the internal features of the material itself. These actions are analogous to the behavior of light. Ultrasound that is reflected from an internal feature has traveled through the entire thickness of the sample, and is used to make acoustic images. At least three basic types of acoustic microscope have been developed. These are the scanning acoustic microscope (SAM), scanning laser acoustic microscope (SLAM), and C-mode scanning acoustic microscope (C-SAM).

C-SAM uses the same transducer to pulse ultrasound and receive the return echoes, meaning that the acoustic image can easily be constrained to a depth of interest. It has the ability to create images by generating a pulse of ultrasound focused to a pinpoint spot. The pulse is sent into a sample and reflected off of interfaces (see Figure 2). The frequency of the pulse and design of the lens are chosen to optimize spot size resolution and depth penetration for each application. In the reflection mode of operation the same transducer is used to send and receive the ultrasonic pulse. Return echoes arrive at different times based upon the depth of the reflecting feature and the velocity of sound in the materials. The operator positions an electronic gate to capture the depth of interest. The amount of ultrasound reflected at the interface is based on the differences in the materials at the interface. The more different the materials the more ultrasound reflected.

Similar to x-ray, acoustic microscopy is a non-destructive technique for visualization of defects, widely used in the production of electronic components and assemblies for quality control, reliability and failure analysis. Usually the interest is in finding and analyzing internal defects such as delaminations, cracks and voids, although an acoustic microscope may also be used simply to verify (by material characterization or imaging, or both) that a given part or a given material meets specifications or, in some instances, is not counterfeit. Acoustic microscopes are also used to image printed circuit boards and other assemblies.

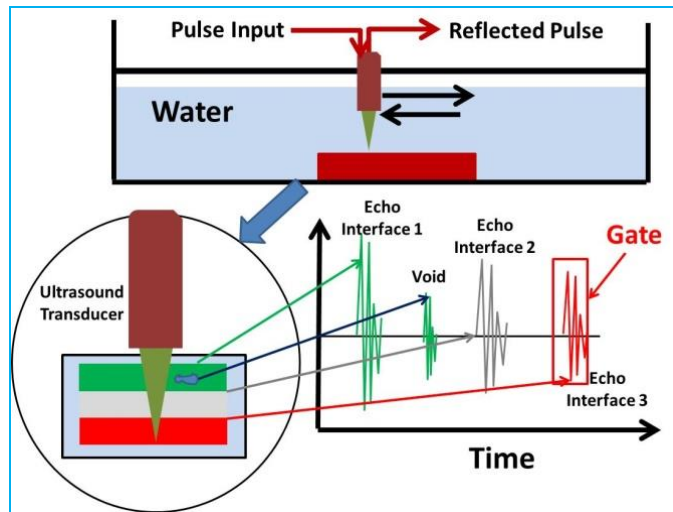


Figure 2. Key features of C-SAM operation and detection of defects including voids and delamination.

The ultrasonic frequencies pulsed into samples by the transducers of acoustic microscopes range from a low of 10 MHz (rarely, 5 MHz) to a high of 400 MHz or more. Across this spectrum of frequencies there is a trade-off of penetration and resolution. Ultrasound at low frequencies (such as 10 MHz) penetrates deeper into materials than ultrasound at higher frequencies (see Figure 4), but the spatial resolution of the acoustic image is less. On the other hand, ultrasound at very high frequencies does not penetrate deeply, but provides acoustic images having very high resolution. The frequency chosen to image a particular sample will depend on the geometry of the part and on the types of materials.

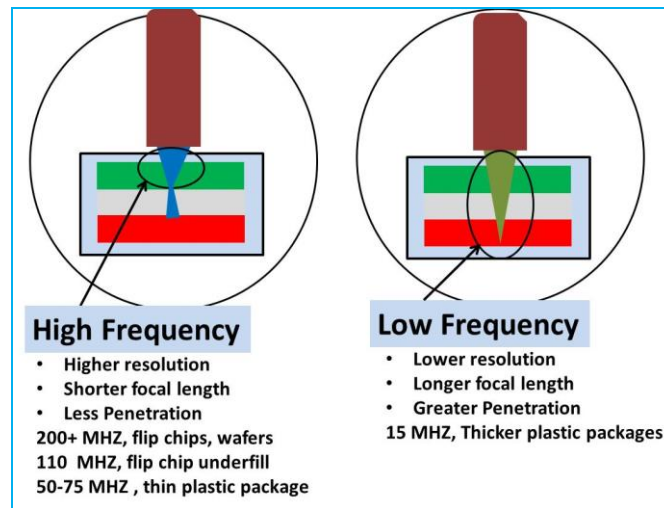


Figure 3. Selection of appropriate transducers is key in optimizing penetration and resolution for the flip-chip BGA and CGA.

Figure 4 schematically compares a few features of flip chip CGA/BGA detectable by AMI and x-ray. X-ray uses high-energy electromagnetic radiation with shorter wavelengths than ultraviolet light to detect inner features. They are highly penetrable depending on the x-ray's energy, which increases with frequency. As frequency and thus penetration increase, the type of x-ray moves from "soft" to "hard." The reflective nature of AMI allows for detection of delamination, whereas the penetration of x-ray allows detection of both short and large voids. These two inspection approaches are complementary techniques that should be used to reveal different features. The x-ray technique relies on the differential attenuation of x-ray energy, whereas the AMI technique relies on material change. The practical result is that AMI is orders of magnitude more sensitive for detecting air space type defects such as voids, delaminations and cracks.

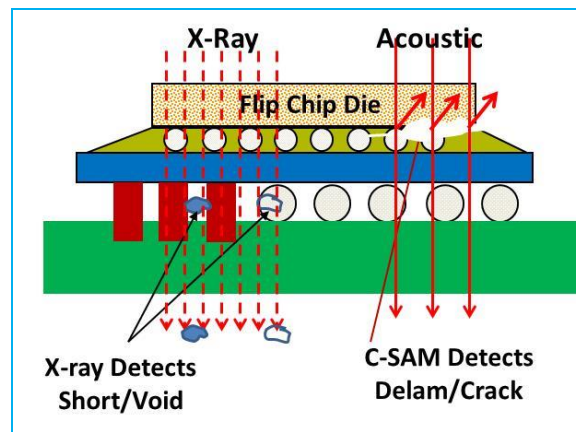


Figure 4. Key features of defect detectability by x-ray and C-SAM for flip-chip BGA/CGA.

1.3 AMI for Microelectronics Inspection Applications

In a previous comprehensive study, Sandor and Agarwal [7] utilized the C-SAM nondestructive technique to evaluate commercial-off-the-shelf (COTS) plastic encapsulate microcircuit (PEM). Samples from different commercial vendors were used for detecting internal defects due to various environmental exposures. PEM failure modes reported in industry due to delamination are summarized as:

- Stress-induced passivation damage over the die surface
- Wire-bond degradation due to shear displacement
- Accelerated metal corrosion
- Die-attach adhesion
- Intermittent electrical signals at high temperature
- Popcorn cracking
- Die cracking
- Device latch-up

Figure 5 shows one of the most common failure modes (popcorning) as a result of delamination, moisture accumulation, and pressure release within a plastic package during the board assembly process. Delamination is dependent on package construction, package size, die size, lead design, number of leads, and environmental stresses, among other influences.

Sandor and Agarwal reported a number of anomalies and potential reliability defects including delamination at die attach, at leads within the mold compound, around the die within the mold compound, on top of the die, and at the backside of the die paddle. The authors analyzed the defect anomalies by C-SAM imaging to determine their impact on the reliability of PEMs. C-SAM images from the beginning of a screening flow were used as a predictor of good or poor subsequent electrical performance of devices. Images tended to correlate with changes in electrical performance. C-SAM inspection and electrical parametric shifts of devices that were subjected to convection reflow were affected less than those equivalent devices exposed to hand soldering and vapor phase reflow (two zones, preheat and reflow).

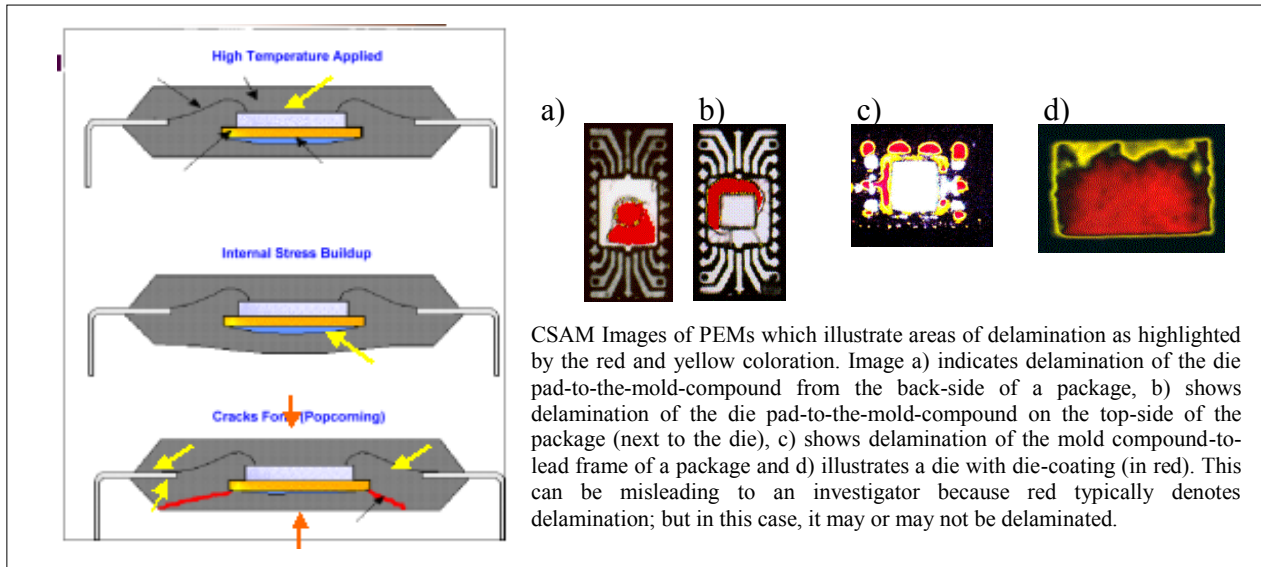


Figure 5. Examples of packages with delamination. The yellow arrows show areas where the existence of delamination can accelerate entry/collection of moisture; the red lines show where the cracks (popcorning) typically occur when the board is exposed to high temperature during assembly [7].

In an investigation of defect detection for a multilayer ceramic capacitor (MLCC) [8], it was found that the 50-MHz transducer is more effective in detecting defects during screening by C-SAM than a 30-MHz version. Screening at a higher frequency enabled reducing rejection that was initially discovered during the board level testing. It saved costly rework at the board level even though there was a slight cost increase due to additional MLCC rejection.

AMI has been used also to analyze flip chip underfill and interconnect bonds since early 2000 when ultra-high frequency transducers are introduced [9]. It was shown that defects such as delamination and void can be detected at each layer and, with 3V (virtual volumetric viewing), the 3D morphology and depth location of the defects can give important information as to the cause of the flaws. Transducers and imaging techniques provided focused access of the ultrasound beam to the interface of interest (chip/ bump and underfill, or bump and underfill/substrate) through any thickness of silicon commonly encountered.

Kessler [10] has shown using color acoustic images, full or partial disband of solder balls and voids in the underfill in a flip-chip assembly. To show such conditions, a flip-chip package was imaged from the top side from the back of the die at the high acoustic frequency of 230 MHz using a high resolution scan of 1024x960 pixels. Gating, region of set AE echo, was on the interface between the die face and the underfill material; therefore, the condition of bonding pads onto the die face was revealed. In another case, the flip-chip package was imaged from the bottom substrate side. Gating was on the interface between the cured underfill and the substrate; therefore bonding the solder balls to their pads. This shows difficulty of implementing such condition for a real application when a large number of other package and materials interfere with acoustic signals.

Sakuma, et al. [11] used non-destruction techniques for flip-chip improvement as well as verification for such improvement. Both C-SAM and x-ray NDE images were presented for an assembly prior to its optimization by a differential heating/cooling chip joint method. The C-SAM investigation detected fractures in the ULK layers, whereas x-ray techniques identified solder joint bridging. In a recent investigation, Phommahaxay et al. [12, 13] stated that even though the 200 MHz transducer can detect gross defects, it does not have sufficient resolution to detect voids in a through silicon vias (TSV). Micron size defect detection required the development of a C-SAM transducer with 1 GHz capability. Such a high frequency transducer allowed good and bad TSVs to be distinguished in a number of test samples. The new SAM with resolution and depth sensitivity and defect resolution $\gg 10 \mu\text{m}$ range enables localization and measure of defects in z- 3 D approach. So,

new GHz SAM can be utilized as a new approach for semiconductor failure analysis in 1 μm range with potential for in line tool TSV inspection development for complete 300 mm wafer inspection

2.0 EXPERIMENTAL EVALUATION BY C-SAM

2.1 Test Plan and Evaluation Approaches

This section covers evaluation performed by C-SAM using a number of advanced packages and assemblies before and after various environmental exposure. Representative flip-chip plastic and ceramic area array (ball/column) packages and assemblies from the previous investigations were subjected to C-SAM evaluation. It also included recently acquired land grid array packages and fine pitch assemblies. Key packages evaluated included are:

- A plastic land grid array after assembly. Because of extremely low stand-off, it was extremely difficult to visually inspect solder interconnections. It was thought that C-SAM technique may provide an insight into integrity of solder interconnections.
- A ceramic flip-chip LGA package with 1517 I/O, which were previously assembled onto PCB and then removed, was subjected to C-SAM evaluation. So, the flip-chip die was exposed to two reflow cycles. Since the flip-chip die had no heat sink attachment, its back was exposed. Also, a CGA assembly version of this LGA package, which were previously assembled onto PCB and subjected to thermal cycling, was included in the C-SAM evaluation.
- A flip-chip CGA1752 I/O package assembly was also subject to C-SAM evaluation. It was realized that this package has an extra heat sink attachment; therefore, the acoustic signal from bonding materials will be a dominant signal.
- A flip-chip BGA1704 I/O package assembly was also subjected to C-SAM evaluation. The flip-chip die of this package, similar to its ceramic CGA 1752 counterpart, also had an extra interface due to heat sink attachment. This package assembly previously was subjected to a number of thermal cycles.
- The FC-CGA 1752 I/O after its heat sink was removed was re-examined. This CGA was re-evaluated by C-SAM for integrity of the flip-chip solder joints since original package showed only integrity of heat sink bonding materials.
- A hermetically sealed CGA with 1272 columns, which had die wire bonded, was also subject to C-SAM evaluation to determine if internal integrity of wire bonds could be assessed.
- A large number of fine pitch and stack package assemblies were subjected to C-SAM to evaluate their integrity and appropriateness of C-SAM.
- The FC-CGA 1752 package with no heat sink along with a fine pitch package was subjected to cycles up to 20 times of solder iron touch to induce defects. These were re-scanned to determine the level of damage and their detectability by the C-SAM technique.
- Cross-sectional examinations were performed for the LGA 1517 I/O to correlate the C-SAM images with optical microscopy images.

To achieve the highest results with limited funding, this investigation examined only packages as individual or test vehicles built previously, either used samples “as assembled” or were already subjected to thermal cycling conditions. Ideally, new test vehicles with inducing known defects should add additional values when additional funds become available. The purpose of using such a mix of packages and assemblies was to initially determine the benefits of C-SAM and to determine its potential limitations, especially for FCBGA and FC-CGA. Detailed information on package including internal configuration, optical photomicrographs, x-ray and as well C-SAM images using a range of transducers are also presented. Two facilities one external and one internal were used for the C-SAM evaluation. The outside facility had extensive equipment capability with an experienced operator, whereas the internal C-SAM equipment had a lower capability with a less experienced operator. Results are presented.

2.2 Plastic LGA132

Figure 6 compares an optical photomicrograph image of a plastic LGA package assembly with 132 lands and their x-ray and C-SAM images. The C-SAM image was taken using a very low frequency transducer of 5 MHz in order enable deeper acoustic wave penetration into the package for comparison to its x-ray images. The C-SAM image shows a few key internal chips similar to x-ray, but several other details are missing. The x-ray shows greater details of internal package configuration,

including solder on land pads and land shape (e.g., a square land on the top left). Layering image is impossible with the 2D x-ray, but it can be performed by the C-SAM technique. Figure 7 shows C-SAM layering images using a 25 MHz transducer. It clearly shows different interfaces in package assembly from the top to the bottom.

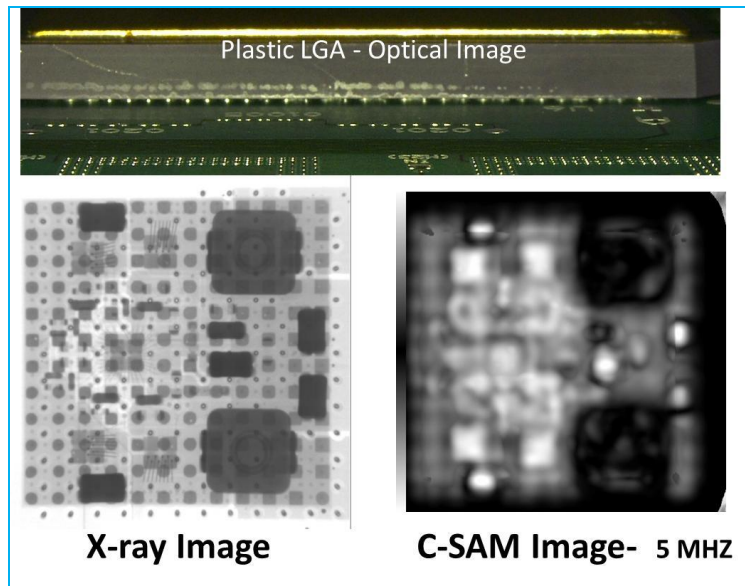


Figure 6. Comparison images by optical microscopy (top), by x-ray (bottom left) and by C-SAM from the LGA 132 I/O assembly.

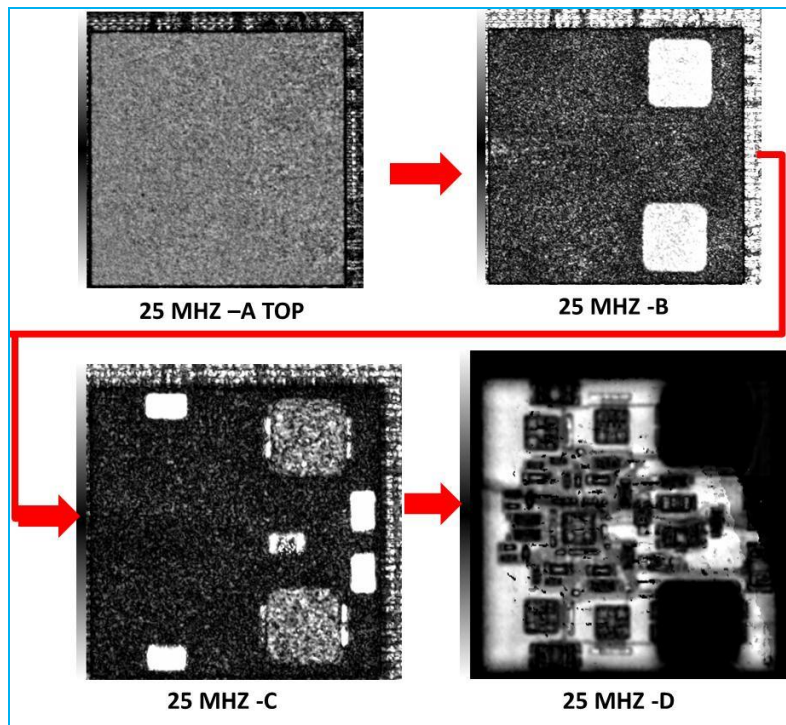


Figure 7. C-SAM layering images taken from the top to the internal LGA package assembly.

2.3 Flip-Chip BGA1704 with Heat Sink

The cross-sectional photomicrograph from a FCBGA1704, which was previously subjected to a number of thermal cycles, is shown in Figure 8. It is apparent that the back of the flip-chip die is covered by a heat sink that extended over the edge of the die, covering the flip-chip area. The only feature that could be revealed through C-SAM evaluation was the bonding

condition of the thermal interface material (TIM). No information regarding underfill or solder bump condition below the TIM could be revealed due to this interface interference with the layers of interest. Hence, the heat sink hindered C-SAM evaluation.

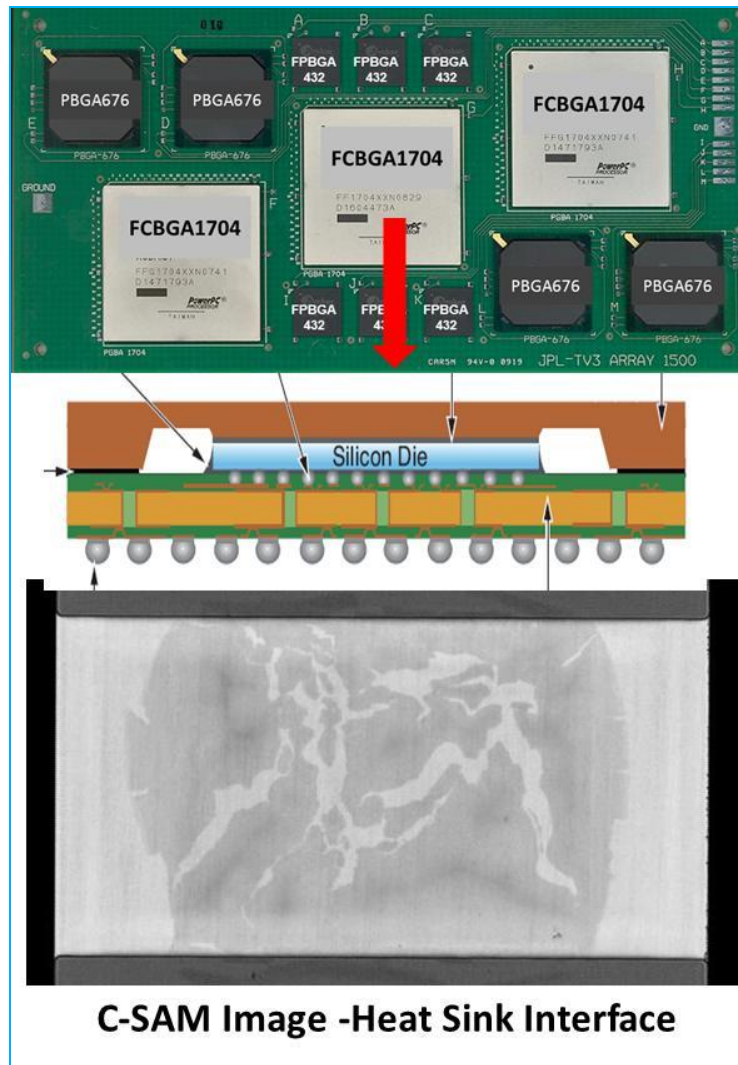


Figure 8. C-SAM image for plastic FC-BGA 1704 I/O assembly showing the heat sink interface, which hindered further penetration of signals.

2.4 Flip-Chip CGA1752 with Heat Sink

The schematic drawing of FC-CGA1752 is illustrated in Figure 9. It is apparent that this package has an additional heat sink that overshadows the flip-chip die, explaining the C-SAM signal interference with the TIM interface. Due to the TIM interference, no layering imaging was possible. The heat sink restricted the C-SAM evaluation.

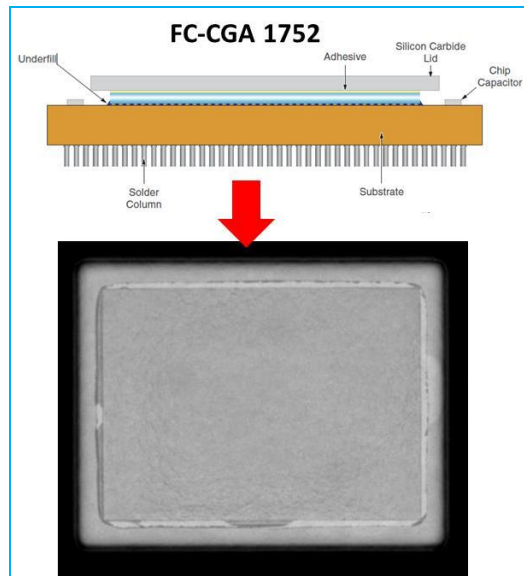


Figure 9. C-SAM image for FC-CGA 1752 I/O assembly showing heat sink interface, which hinders further penetration of signals.

2.5 Flip-Chip LGA1517/CGA without Heat Sink

This ceramic LGA package was ideal for revealing the integrity of the flip-die, since its heat sink was yet to be attached. Two styles of LGAs with 1517 I/Os were evaluated; one as a package and the other as an assembly. Irrespective of the package being alone or in an assembly, there was no heat sink and the back of the flip-chip die was exposed. There was no C-SAM signal interference due to the TIM as it was the case for CGA 1752 I/O. The first interface was between the die and solder bump and underfill. The second was between substrate and the land pads or solder joints of columns. Figures 10 to 12 show three C-SAM images taken with three different transducers with increasing frequencies of 25-, 100-, and 230-MHz. It is apparent that as frequency increases the granularity of the C-SAM image increases due to increase in spatial resolution. The details of the flip-chip solder bumps became apparent at a higher frequency. There is a dark region, which is surrounding the central white region. The dark area is postulated to be a total separation of underfill, but needs to be verified. A similar separation condition was also observed for the other LGA 1517 I/O package assembly (SN041), as shown Figure 13

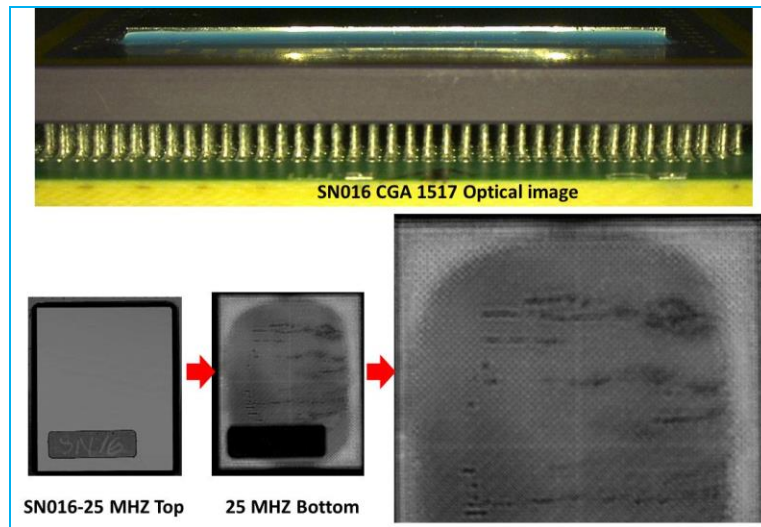


Figure 10. Optical and C-SAM (at 25 MHz) layering images for FC-CGA 1517 assembly (SN016) showing flip-chip top and flip chip bump interface. This package had no heat sink.

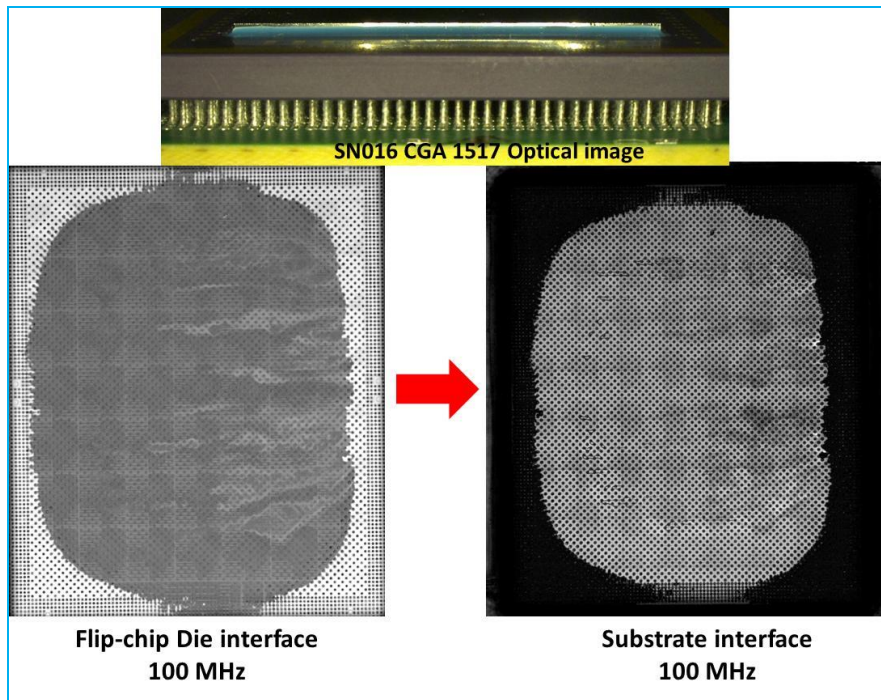


Figure 11. Optical and C-SAM (at 100 MHz) images for FC-CGA 1517 assembly (SN016) showing images for die and substrate interfaces.

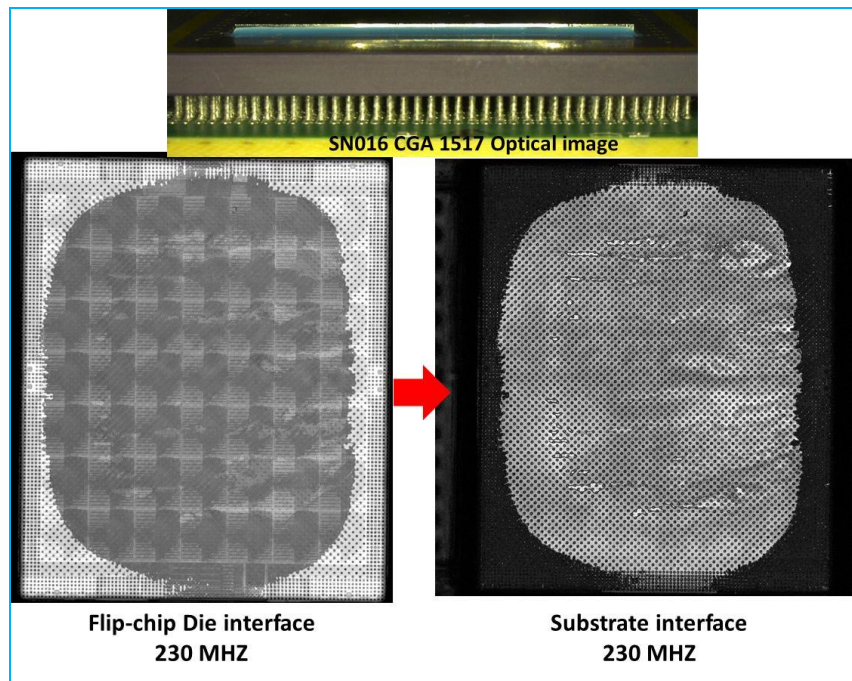


Figure 12. Optical and C-SAM (at 230 MHz) images for FC-CGA 1517 assembly (SN016) showing images for die and substrate interfaces.

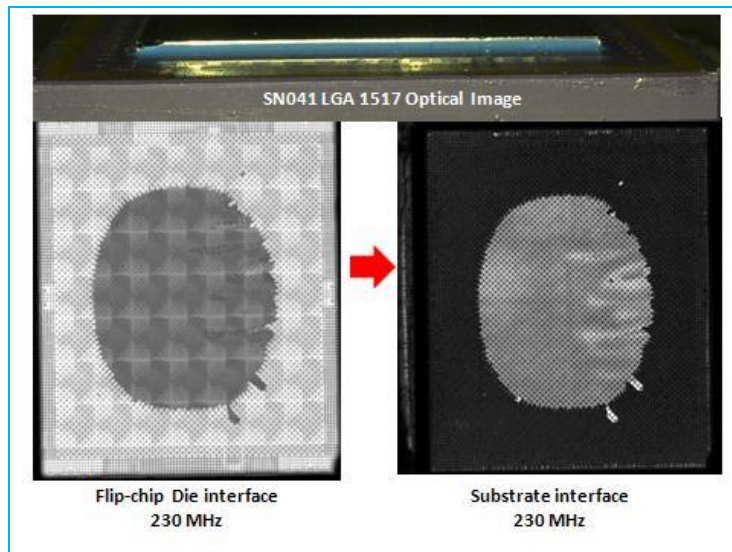


Figure 13. Optical and C-SAM (at 230 MHz) images for FC-CGA 1517 assembly (SN041) showing images for die and substrate interfaces.

2.6 Fine Pitch PBGAs 432 and 676 I/O

Two plastic ball grid array package assemblies, one with 432 balls and 0.4-mm pitch and the other with 676 balls and 1-mm pitch, were subjected to C-SAM evaluation. Figure 14 shows the C-SAM images for these packages as well an optical picture of the test vehicle and the package assemblies. Generally, the C-SAM method is recommended for inspection of individual packages before assembly. Prevalent delamination and “popcorn” cracking in PBGA can be detected. Nevertheless, a few features of packages such as die configuration and outline, as well as attachment condition with no signs of popcorn delamination, could be identified. However, the integrity of solder ball attachment and solder joints on the board are unidentifiable. Multiple interfaces hinders accurate C-SAM evaluation of hidden solders under the package.

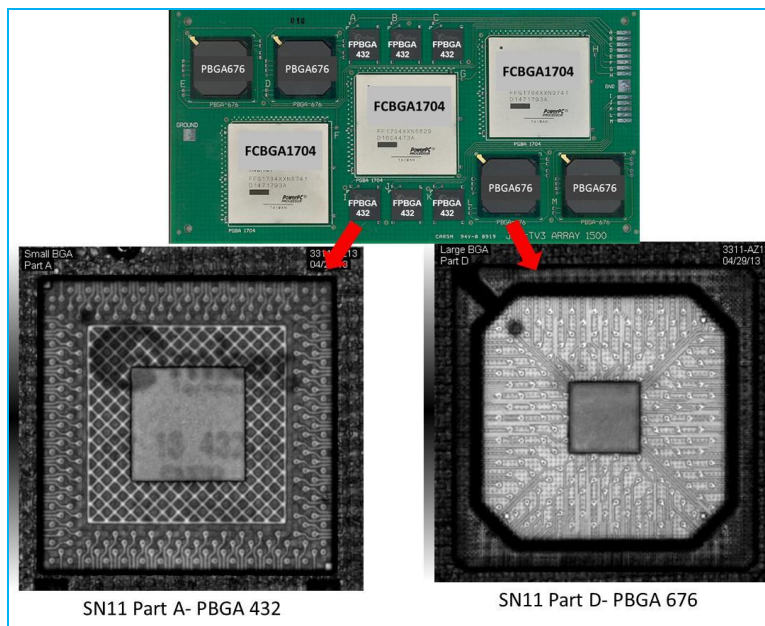


Figure 14. Optical and C-SAM images for fine pitch PBGA 432 I/O and PBGA 676 I/O.

2.7 C-SAM Repeat of CGA1752 after Heat Sink Removal

The initial C-SAM evaluation of FC-CGA 1752 I/O did not reveal the condition of the flip-chip die and underfill due to the package having a heat-sink interface. We successfully disbonded the heat from the die using a lap shear testing approach. The section of the flip-chip die with no heat sink was subjected to C-SAM evaluation to determine the condition of the flip-chip

die and underfill. Figure 15 shows one optical and two C-SAM images of the CGA package. The condition of the flip-chip solder balls and joints appears to be acceptable. Only a small anomaly was detected in the underfill at the center of flip-chip die, as indicated by the arrow. To induce additional defects, this flip-chip CGA with no heat sink was subjected to 20 solder iron touches with a tip temperature of 700°F, each for about 5 seconds. No additional defects were detected. Other means need to be developed to induce controlled defects and evaluation by C-SAM.

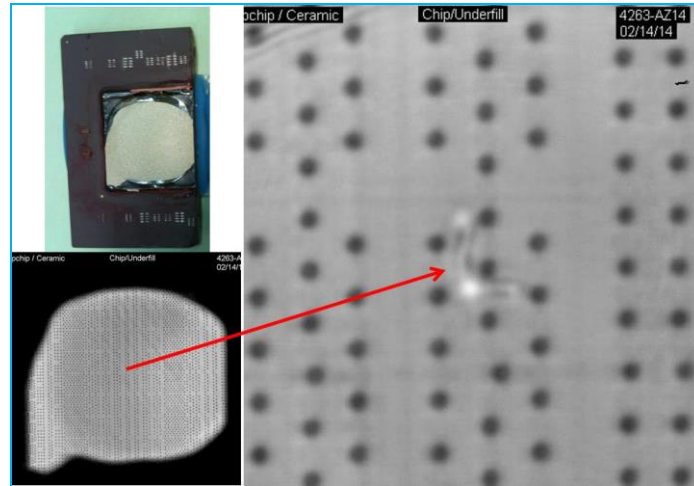


Figure 15. Optical (top left) and C-SAM images for FC-CGA 1752 I/O assembly after removal of the heat sink, showing the integrity of the flip-chip assembly and minor defect anomaly.

2.8 Hermetically Sealed CGA1272 with Internal Wire Bonds

Figure 16 shows a C-SAM image of a CGA1272 I/O package assembly. Only outer surfaces including the lid brazing section could be detected by C-SAM.

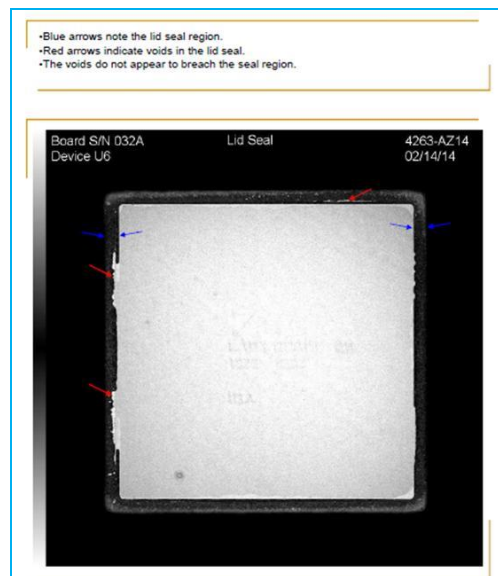


Figure 16. C-SAM images for a hermetically sealed CGA 1272 I/O assembly showing heat sink seal integrity. Blue arrows shows the lid seal region and red arrows show areas with voids.

2.9 Plastic LGA 1156 I/O and Fine Pitch Package Assemblies

Plastic LGA with 1156 I/O were subjected to C-SAM evaluation. Figure 17 shows images of this package. No defect anomaly was detected by C-SAM. Characterization was limited to the top section only. A number of other fine pitch plastic packages were also imaged. No defect anomaly was detected.

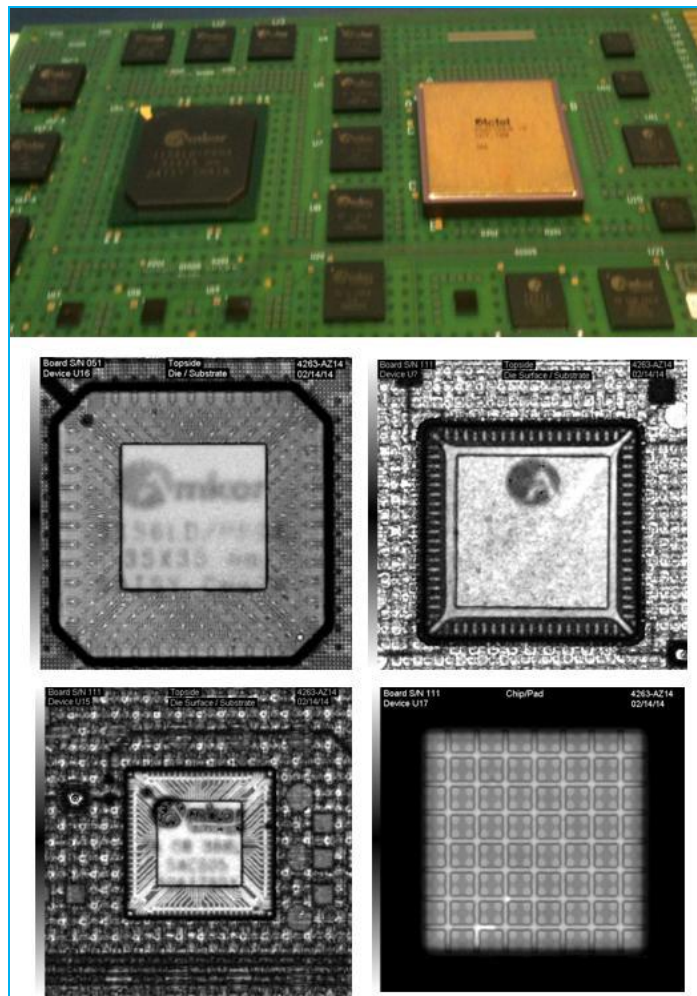


Figure 17. Optical (top) and representative C-SAM images for various PBGA and FPGA package assemblies.

2.10 Effect of 20 Solder Iron Touches at 700°F

CGA 1752 I/O without heat sink and one fine pitch plastic BGA package assembly was subjected up to 20 solder iron touches at 700°F, each for about 5 seconds. C-SAM was performed at 5, 10, and 20 exposures. Figure 18 shows C-SAM images after twenty touch ups. No anomaly was detectable for either package after 20 touches.

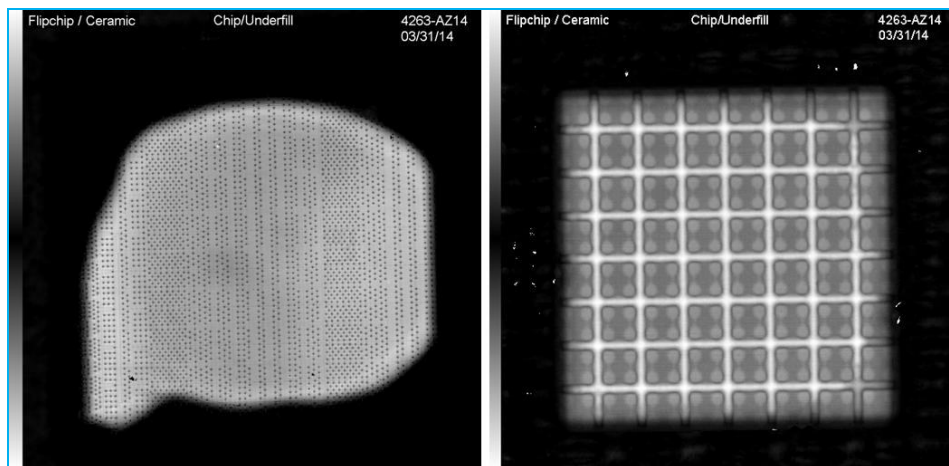


Figure 18. C-SAM images for FC-CGA 1752 I/O and FPBGA after 20 touches with a solder iron with 700°F tip temperature. No apparent changes were revealed.

2.11 Cross-sectional Characterization of LGA1517

The flip-chip ceramic LGA1517 package was cross-sectioned to verify the condition of solder bump solder joints and underfill integrity. This package was selected for X-sectioning since it clearly showed a large dark area on the periphery of the die with minor shadowing at the center of the die. Figure 19 shows the optical image of X-sectioned LGA package at lower and higher magnifications. Inspection of the X-sectioned samples did not reveal any separation in the periphery of the die, as revealed by the C-SAM images. The reason for this discrepancy is unknown.

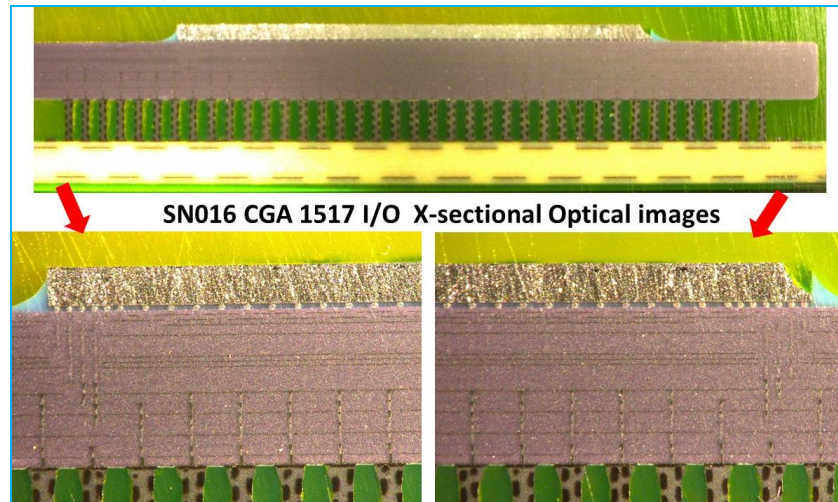


Figure 19. Optical image of a microsection of FC-CGA 1517 assembly (SN016), showing images for die and underfill.

3.0 CONCLUSIONS

The evaluations covered in this paper deal with inspection methods and comparison of inspection results performed for advanced flip-chip column grid array, flip-chip ball grid, and a number of other fine pitch ball grid array and land grid array package assemblies. Visual inspection using optical microscopy has been the traditional approach for acceptance/rejection of workmanship defects by quality assurance personnel. Inspection of hidden elements in FC-CGA and FCBGA package assemblies requires using nondestructive inspection tools such as 2D/3D x-ray and, potentially, acoustic microscopic imaging. Limitations on using acoustic emission for solder joint assemblies are yet to be fully established.

AE and x-ray are complementary techniques that are frequently found in the same laboratories, but they reveal different features. X-ray detects features based on differential attenuation of the x-ray energy, whereas AE detects features based on materials changes. The practical result is that AE is orders of magnitude more sensitive for detecting air-gap defects such as voids, delaminations and cracks. C-mode scanning acoustic microscopy was evaluated for advanced electronic packaging assemblies, particularly FC-CGA and FCBGA. Inspection evaluations revealed the following results.

- Visual inspection by optical microscopy is ideal for detecting exposed features such as dewetting, microcracks, cold, and disturbed solder joint.
- Visual inspection is possible for periphery columns in CGA and balls in BGA, but is difficult for joints in a plastic land grid array due to a lower gap height. A 2D x-ray revealed many internal features of the LGA package including chips and solder joints.
- Layering C-SAM using a low frequency transducer revealed many features of the plastic LGA package assembly detected by x-ray; however, the features were less clear and it did not reveal package and board interfaces or solder joint conditions.
- It was revealed that C-SAM could only show the quality of heat-sink thermal interface bonding materials of the FC-CGA 1752 I/O. Heat sink is part of the package and is attached with adhesive on top of the flip-chip die, hence, it hindered penetration by acoustic emission signal into bumps and adhesive interfaces.
- C-SAM revealed the flip-chip bumps and underfill conditions of the FC-CGA package after shearing off its heat sink.

- The C-SAM revealed an edge delamination for FC-CGA 1517 I/O assembly since it had no heat sink on the flip-chip die. This allowed C-SAM characterization of the flip-chip bumps and underfill materials.
- Microscopic cross-sectional evaluation of FC-CGA 1517 did not support the edge-delamination revealed by the C-SAM images.
- C-SAM of a hermetically sealed LGA 1272 package revealed only the lid bonding defects. Internal features could not be detected. For plastic LGA1156, the C-SAM revealed only the die, but not the solder joint condition.
- C-SAM of a large number of other fine pitch ball grid array assemblies revealed internal die integrity and configuration, but it did not show solder ball or joint attachment integrity.
- No defect was detected by C-SAM when CGA 1752 I/O and fine pitch BGA packages with 20 repeated solder iron touches, each for about 5 seconds using a tip temperature of 700°F.

Non-destructive evaluation of microelectronic packaging and assemblies is of critical importance in assuring reliability. Understanding key features of various NDE inspection systems in detecting defects in the early stages of assembly are critical to developing approaches that will minimize future failures. Additional specific, tailored, NDE inspection approaches could enable low-risk insertion of these advanced electronic packages.

Even though C-SAM showed significantly lower versatility in defect detection compared to x-ray for packages and assemblies of FC-CGA and FCBGA, the C-SAM techniques are widely used for detection of flip-chip die attachment by package manufacturers during the early stages of the flip-chip die assembly. However, added additional interfaces, e.g. heat sink on die, limits the use of acoustic emission approach at package and assembly levels. The recently developed GHZ SAM version is shown to have potential for TSV defect detection even for complete wafer inspection.

C-SAM inspection is a non-destructive technique with a wider use for revealing hidden gap defects, including delamination and voids. It is recommended that the C-SAM characterization be used as a complement to other inspection techniques, including x-ray and traditional visual inspection by optical microscopy. It is apparent that a combination of various inspection techniques may be required in order to assure quality at part, package, and system levels. This is especially true for newly introduced miniaturized advanced electronic packages with hidden flip-chip solder bumps at the die level and solder balls at the package level with associated underfill and solder joints.

4.0 ACKNOWLEDGMENTS

This research was carried out at the Jet Propulsion Laboratory, California Institute of Technology, and was sponsored by the National Aeronautics and Space Administration Electronic Parts and Packaging (NEPP) Program.

Reference herein to any specific commercial product, process, or service by trade name, trademark, manufacturer, or otherwise, does not constitute or imply its endorsement by the United States Government or the Jet Propulsion Laboratory, California Institute of Technology. ©2015. California Institute of Technology. Government sponsorship acknowledged.

The author would like to acknowledge many people from industry, especially Ken Tylor, and the Jet Propulsion Laboratory (JPL), especially Steve Bolin, who were critical to the progress of this activity. The author extends his appreciation to program managers of the National Aeronautics and Space Administration Electronics Parts and Packaging (NEPP) Program, including Michael Sampson and Ken LaBel for their continuous support and encouragement.

References

- [1] Ghaffarian, R., “Damage and Failures of CGA/BGA Assemblies under TC and Dynamic Loading,” ASME, IMEC, San Diego, CA, Nov. 2013
- [2] Ghaffarian, R. “Thermal Cycle and Vibration/Drop Reliability of Area Array Package Assemblies,” *Structural Dynamics of Electronics and Photonic Systems*, eds. E. Suhir, E. Connally, and D. Steinberg, Chapter 22, John Wiley, New York, NY, 2011.
- [3] Ghaffarian, R., “Thermal Cycle Reliability and Failure Mechanisms of CCGA and PBGA Assemblies with and without Corner Staking,” *IEEE Transactions on Components and Packaging Technologies*, Vol. 31, Issue 2, 2008.
- [4] Ghaffarian, R. “CCGA Packages for Space Applications,” *Microelectronics Reliability* **46** 2006–2024, 2006.
- [5] Fjelstad, J., Ghaffarian, R., and Kim, Y.G., *Chip Scale Packaging for Modern Electronics*, Electrochemical Publications, 2002.
- [6] <http://www.sonoscan.com/technology/ami-basics1-3.html>, Accessed Jan 27, 2014
- [7] Sandor, M., Agarwal, S., “Using Nondestructive Methods (C-SAM) for COTS PEMs Screening and Qualification,” CMSE, Feb. 2001, <http://trs-new.jpl.nasa.gov/dspace/bitstream/2014/39431/1/01-0006.pdf>, Accessed Jan. 27, 2014
- [8] Kostic, A.D., Schwartz, S.W., “Optimized Acoustic Microscopy Screening for Multilayer Ceramic Capacitors,” Proceedings of Reliability and Maintainability Symposium (RAM), 2011, Pages :1-4
- [9] Semmens, J. “Flip Chips and Acoustic Micro Imaging: An Overview of Past Applications, Present Status, And Roadmap for the Future,” <http://www.sonoscan.com>, Accessed Jan 27, 2014
- [10] Kessler, L.W., “Probing Flip-Chip Interfaces,” Mar. 1, 2006, <http://www.edn.com/design/test-and-measurement/4381152/Probing-flip-chip-interfaces>, Accessed Jan 27, 2014
- [11] Sakuma, K., Smith, K., Tunga, K., Perecto, E., Wassick, T., Pompeo, F., Nah, J., “Differential Heating/Cooling Chip Joining Method to Prevent Package Interaction Issue in Large Die With Ultra Low-K Technology,” Electronic Components and Technology Conference (ECTC), 2012
- [12] Phommahaxay, A., et al, “High Frequency Scanning Acoustic Microscopy Applied to 3D Integrated Process: Void Detection in Through Silicon Vias,” Electronic Components and Technology Conference (ECTC), 2013
- [13] Czurratis, P., Djuric, T., Hoffrogge, P., Phommahaxay, A. De Wolf, I., “New Scanning Acoustic Microscopy Technologies Applied to 3D Integration Applications,” <http://www.nist.gov/pml/div683/conference/upload/czurratis.pdf>, Accessed, Nov. 21, 2015

6.0 ACRONYMS AND ABBREVIATIONS

2D	two-dimension	NASA	National Aeronautics and Space Administration
3D	three-dimension	NDE	nondestructive evaluation
3V	virtual volumetric viewing	NEPP	NASA Electronic Parts and Packaging
AE	acoustic emission	PBGA	plastic ball grid array
AMI	acoustic microimaging	PCB	printed circuit board
BGA	ball grid array	PEM	plastic encapsulated microcircuit
CBGA	ceramic ball grid array	PWB	printed wiring board
CCGA	ceramic column grid array	QA	quality assurance
CGA	column grid array	ROHS	restriction on hazardous substances
COTS	commercial-off-the-shelf	SAM	scanning acoustic microscope
CQFP	ceramic quad flat pack	SLAM	scanning laser acoustic microscope
C-SAM	C-mode scanning acoustic microscopy	TIM	thermal interface material
ESD	electrostatic discharge	TSV	through silicon via
FC	flip chip	ULK	ultra low-K
FCBGA	flip-chip ball grid array	X-section	cross-section
FC-CGA	flip-chip column grid array		
I/O	input/output		
JPL	Jet Propulsion Laboratory		
LGA	land grid array		
MIP	mandatory inspection point		
MLCC	multilayer ceramic capacitor		